Fibers and Polymers 2021, Vol.22, No.5, 1366-1377
DOI 10.1007/s12221-021-0570-4

ISSN 1229-9197 (print version)
ISSN 1875-0052 (electronic version)

Synthesis Effect of Nano-fillers on the Damage Resistance of GLARE

M. Megahed*, M. A. Abd El-baky, A. M. Alsaeedy, and A. E. Alshorbagy

Department of Mechanical Design and Production Engineering, Faculty of Engineering, Zagazig University, Zagazig 44519, Egypt

(Received May 18, 2020; Revised July 17, 2020; Accepted July 23, 2020)

Abstract: GLARE (glass reinforced aluminum laminate) is applied in the aerospace and in vehicle structures. Degradation and failure in these applications commonly initiate at the location of cracks and joints. To improve the damage resistance of GLARE against stress concentration presented in the vicinity of the hole and around the crack tip, GLARE has been filled with different types of nano-fillers. Aluminum (Al) skin layers were treated to achieve good bonding between Al-sheets and nanocomposite laminate. Results showed that a maximum enhancement of 26.3 %, 35 %, and 22.6 % in bearing strength, in-plane shear strength, and fracture toughness, respectively, was attained by the inclusion of silica nano-filler to GLARE. Adding alumina to GLARE also causes an enhancement in these properties in a good manner. An improvement of 21.6 %, 28.7 %, and 20.7 % was obtained in bearing strength, in-plane shear strength, and fracture toughness, respectively, as compared to pristine GLARE. Other nano-modified GLARE laminates showed an improvement in bearing strength, in-plane shear strength, and fracture toughness as compared to pristine GLARE. However, adding nanoclay has an adverse effect. The elemental map showed a uniform distribution of alumina nano-filler into the epoxy matrix, which reveals the enhancement in the mechanical properties.

Keywords: GLARE, Nano-filler, Bearing strength, In-plane shear, Fracture toughness

Introduction

Fiber metal laminates (FMLs) are defined as hybrid composite laminates composed of thin metal alloys sheets and plies of fiber-reinforced polymeric matrices [1,2]. FMLs combine the advantages of metal sheets and fiber/polymer composites [3,4]. An example of FMLs is GLARE which consists of Al-layers and glass fiber/epoxy layers [5]. GLARE is widely applied in the aircraft industry and in automobiles, owing to its better mechanical properties as the damage tolerance behavior [6,7]. Failure in aircraft and automobiles starts at the location of the joints and cracks. Consequently, the resistance to this failure has a strong influence on safety, reliability, and durability.

Until now, mechanical fastening is considered as one of the main ways to join composite components, as no need for surface preparations, easiness in disassembly and inspection [3]. The joints would be predicted to finally fail in different modes that are net-tension, shearing-out, and bearing. In structural design, bearing failure is preferred for the stability of the failure process [8-11]. Bearing failure is considered as a local compressive failure as a cause of contact and frictional forces performed on the surface of the hole [12]. Moreover, shear loads arise in an aircraft fuselage due to bending and torsion. Shear yield strength is important in the design for GLARE that can be obtained through testing [5]. Fiber/ matrix debonding produced by the in-plane shear load is considered one of the major failure modes in composites due to the stress concentration set at the interfaces between fibers and polymeric matrix [13,14]. Furthermore, propagation of a crack tip perpendicular to the direction of fiber reinforcement in FMLs mainly occurs through the Al-sheets and is accompanied by delamination between metal sheets and polymeric matrix. The experimental investigation of the resistance to delamination in FMLs is very essential. The resistance to delamination is well-known as the fracture toughness or fracture resistance [15]. It is desirable for FMLs to exhibit high fracture toughness value, so it has the opportunity to withstand the growth of the cracks through the structure [4].

Recently, nanocomposites have gained much attention owing to the enhancement in physical and mechanical properties when compared to their microcomposites counterparts. This enhancement in properties is due to their high surface area-to-volume ratio relative to larger reinforcements [16-22]. De Villoria *et al*. [23] developed nanocomposites by placing aligned carbon nanotube across each ply-ply interface of carbon-reinforced epoxy composites. The bearing test results show that delamination damage mode is suppressed in the in-plane loaded nanocomposite laminates. An increase of 30 % in the bearing strength was obtained. Likewise, the effect of the inclusion of aluminum oxide nanoparticles on failure modes and loads of glass-epoxy laminate with two parallel pin-loaded holes was investigated [24]. The bearing strength of nanocomposites has been improved. Furthermore, bolted joints were prepared in woven glass fiber/epoxy laminates with the incorporation of nanoclay content from 0 to 5 wt. % [25]. The edge distance to hole diameter ratio and the width to hole diameter ratio were varied from 2-5. An enhancement of 21 % and 35 % was observed for joints with nanoclay having preloads of 3 and 5 Nm, respectively.

*Corresponding author: monawafa6@gmail.com

Kim [26] incorporated carbon nanotubes in woven carbon fiber/epoxy composites to improve their mechanical properties. He reported that the mechanical interlocking between carbon nanotubes and carbon fibers increased the resistance of the nanocomposites to the shear failure. Likewise, Cho *et al*. [27] found that the in-plane shear strength of carbon fiber/epoxy composite filled with functionalized graphene nanoplatelets was enhanced as compared to the neat composites. Also, Khashaba [28] reported that epoxy filled with 0.75 wt. % multi-walled carbon nanotubes has the highest enhancement in the in-plane shear properties as compared to the neat epoxy. Furthermore, the addition of halloysite nanotube to basalt fiber/epoxy composites showed substantial improvement in the fracture toughness and the tensile strength [29]. Furthermore, the fracture tests performed on single-edge-notch bending composites revealed that the inclusion of nanoparticles to epoxy resin can effectively improve the fracture toughness of the composites [30]. Zakaria and Nezhad [31] studied the effect of the modification of epoxy resin in FMLs with mineral nanoclay platelets. Results showed that with the inclusion of 0.5 wt. % of nanoclay, the fracture toughness increases double-fold when compared to the fracture toughness of FMLs without nanoclay. Further inclusion of nanoclay causes a reduction of the fracture toughness. The fracture toughness of FMLs filled with 1 wt. % of nanoclay is slightly beneath FMLs filled with 0.5 wt. % of nanoclay, but it is still upper than unfilled ones. Further inclusion of nanoclay has an adverse influence on the interfacial delamination toughness.

From the above literature survey, many research studied the enhancement in bearing strength, in-plane shear strength, and fracture toughness with adding nano-fillers to polymeric composites. However, studying the influence of adding nano-fillers to the composite part in FMLs is limited. To compensate the influence of the stress concentration and avoid premature failure in the vicinity hole and crack region, reinforcements must be added to the joint [32]. The main challenge in this study is to improve the damage resistance of GLARE with toughening and strengthening the epoxy with the incorporation of different nano-fillers. The influence of the inclusion of 1 wt. % of different nano-fillers to GLARE on bearing, in-plane and fracture toughness properties was investigated. SEM images were used to determine the morphology of unfilled and filled GLARE.

Experimental

Materials

Al-alloy 1050 sheets were used as skin layers in unfilled and filled GLARE. These sheets have a thickness of 0.5 mm and were provided by Metallurgical Industries Company, Egypt. The composite material used in GLARE is composed of ten layers of E-glass woven fiber reinforcement impregnated with epoxy resin. The glass fiber has an areal density of 300 g/m^2 and was provided by Hebei Yuniu Fiberglass Manufacturing Co. Ltd., China. The epoxy used in fabricating the composite core is Kemapoxy 150 RGL. Various nano-fillers were embedded in epoxy with 1 wt. % of epoxy. These nano-fillers are metal nanoparticles as aluminum and copper (Cu) nanoparticles with 70 nm diameter and were provided by US Research Nanomaterials, Inc., USA. Ceramic nano-fillers supplied by Sigma-Aldrich with 20 nm diameter were used as titanium oxide (TiO_2), aluminum oxide (Al_2O_3), and silica (SiO_2). Furthermore, Nanoclay (Nanomer® I.31PS) supplied by Sigma-Aldrich was used. Chemicals like acetone, sodium hydroxide, hydrochloric acid used in the treatment of Al-sheets were provided by El Nasr Pharmaceutical Chemicals, Egypt.

Surface Treatment of Al Alloy Sheets

As delamination between metal sheets and composite laminate is a main issue that affects the performance of GLARE, mechanical and chemical surface treatments of the metallic layers were performed. Mechanical treatment was attained by abrading one side of the Al-alloy sheets by 400 abrasive sandpapers. This side is attached to the composite core. The Al-alloy sheet was wiped by acetone subsequently distilled water. Chemical treatment was obtained by immersing the Al-alloy sheets in a volume of 11 % of the hydrochloric acid solution for 30 min in order to roughen the same side that was treated mechanically. Afterward, the Al-alloy sheets were submerged in a 5 wt. % sodium hydroxide solution at a temperature of 70 ^oC for 5 min then cleaned with distilled water and dried [33].

Fabrication of GLARE Laminates Filled with Nano-fillers

Acetone was used with 10 wt. % [34] as a diluent for epoxy in order to reduce its viscosity which aids in obtaining a good distribution of nano-fillers when embedded in epoxy [35]. Araldite and acetone were stirring manually. Nano-fillers were added gradually with 1 wt. % of epoxy to araldite and acetone. This mixture was first stirred manually then sonicated for 3 hrs with amplitude of 70 % using Hielscher ultrasonic processor (power of 200 watts, frequency of 24 kHz and pulse of 0.5 s on/off cycle). During the sonication process, the mixture was placed in an ice-water bath in order to reduce the emitted temperature. After that the mixture was heated under vacuum furnace at 80 ^oC for 2 hrs to ensure the removal of acetone. Hardener was added to the mixture and was stirred manually thoroughly with a weight ratio of 2:1. Subsequently, hardener was blended for 10 min using magnetic stirrer at 250 rpm to ensure good dispersion of nano-fillers into epoxy and break up aggregation thus the compatibility of nano-fillers with epoxy resin is enhanced [21]. Epoxy was distributed uniformly on the treated side of Al-alloy sheet. Unfilled and filled GLARE laminates were fabricated using woven glass fiber impregnated with epoxy by hand-layup technique

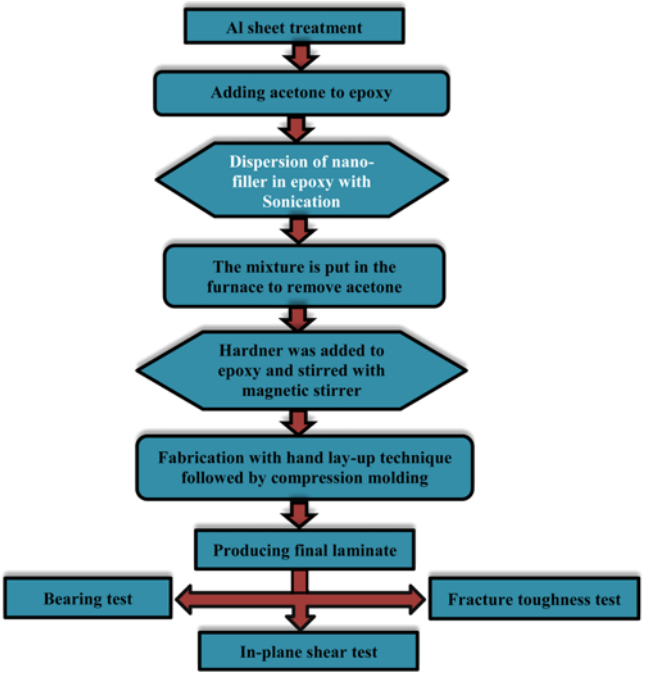

Figure 1. Steps of fabricating of GLARE filled with nano-fillers.

followed by compression molding at a pressure of 1.2 bar. The fabricated GLARE laminates were cured at ambient temperature for 24 hrs under normal conditions. Figure 1 illustrates the steps of fabricating GLARE laminates filled with nano-fillers.

Mechanical Testing

Bearing, in-plane shear, and fracture toughness tests were carried out using Jinan WDW 100 KN universal testing machine. The load-deflection curves were obtained from the computer unit of the universal testing machine. In each test, five specimens of were tested for each type of GLARE and the average value was considered.

Bearing Test

Bearing test was carried out according to ASTM D 5961 on unfilled and filled GLARE specimens at ambient temperature and at a crosshead speed of 2 mm/min. The dimensions of the bearing test specimen are indicated in Figure 2. In bearing test, three basic failure modes can be

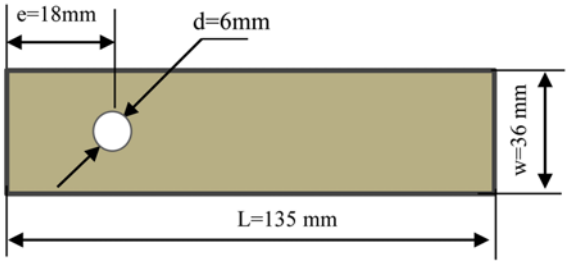

Figure 2. Pinned-joint specimens.

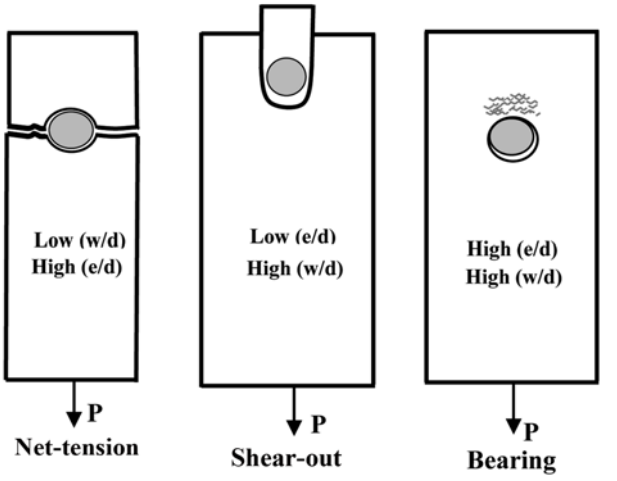

Figure 3. Basic failure modes in bolted laminates.

noticed in the pin-loaded specimen as shown in Figure 3. These failure modes are net tension, shear-out, and bearing. Mixing of these modes also can be noticed. These failure modes depend on the geometric parameters of the joint. These geometric parameters are (e/d) ratio and (w/d) ratio. With low strength, net tension failure mode can be noticed and tension occurs catastrophically. Nevertheless, with high strength, bearing failure mode exists. The optimal strength for metal sheets is produced at an edge distance equal to twice the bolt diameter. In this condition, the joint fails in bearing failure mode, as the hole gradually elongates because of the loading of the fastener. On the contrary, the bearing strength of fiber-reinforced polymer composite is strongly affected by loading direction due to its anisotropic behavior. The anisotropy also cause low bearing strength for a small edge distance, thus edge distance is required to be higher than three times the fastener diameter [32]. Consequently, from a safe design viewpoint, a bearing failure is preferred more than either shear-out failure or net tension failure. As w/d=6, e/d=3 values are selected, bearing is considered the dominant failure mode permitting more progressive damage to arise [36]. Bearing strength (σ_b) can be calculated as follows [37]:

$$\sigma_b = \frac{P}{D_h h} \quad (1)$$

where, P is the failure load, D_h is the bolt or hole diameter and h is the GLARE specimen thickness. The test fixture was fabricated from stainless steel according to the geometry shown in Figure 4. The bolts were neat-fit the hole. In this work, w/d=6, e/d=3 were attained to ensure pure bearing which is safe to unfiled and filled GLARE laminates. GLARE specimen is attached to the pinned-joint fixture as shown in Figure 4.

In-plane Shear Test

In-plane shear tests were performed according to ASTM

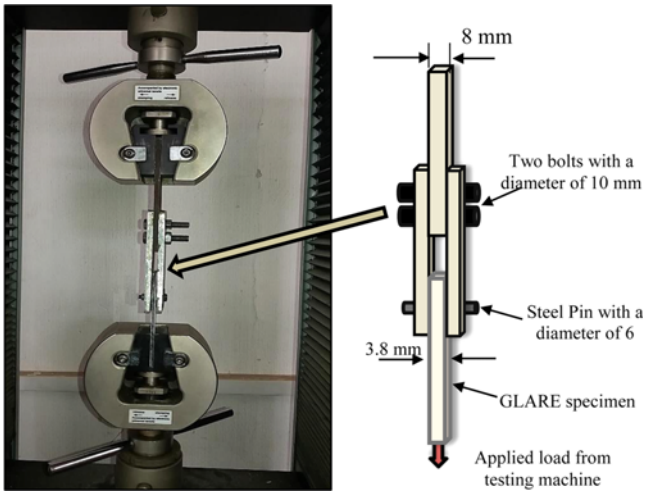

Figure 4. Pinned-joint fixture.

D5379 using Iosipescu test fixture shown in Figure 5(a) at a crosshead speed of 2 mm/min. GLARE specimens were cut into strips with 76 mm length and 19 mm width 90 ° double V-notches were machined at the mid-length of the specimen through its thickness for a depth of 3.8 mm as shown in Figure 5(b). A set of displacements were performed on the V-notch GLARE specimen, so the central area of the GLARE sample is set under pure shear. The displacement is attained through the relative movement of the movable grip as referred to the fixed grip. The in-plane shear strength (τ_{xy}) can be calculated as follows:

$$\tau_{xy} = \frac{P_{max}}{wh} \tag{2}$$

where, P_{max} is the maximum applied load, w is the distance between the roots of the V-notches which is equal to 11.4 mm.

Fracture Toughness Test

Fracture toughness tests were performed according to ASTM D5045. The fracture toughness setup is shown in Figure 6(a). The single end notch bending (SENB) specimens were prepared and then employed in the three-point bending tests. The specimens were tested on the same

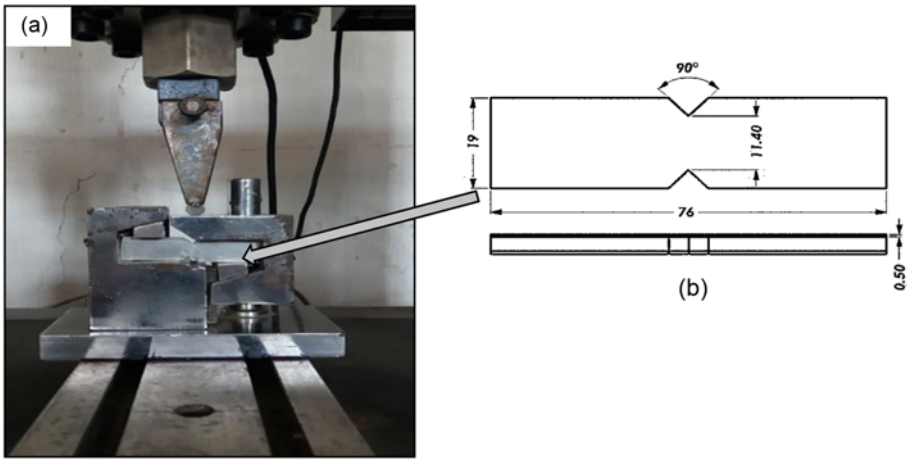

Figure 5. In-plane shear test, (a) Iosipescu test fixture and (b) In-plane shear specimen.

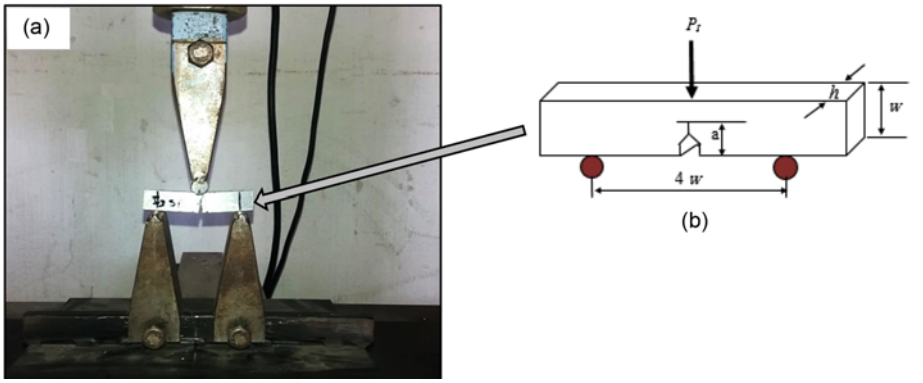

Figure 6. (a) Fracture toughness test set up and (b) SENB fracture toughness GLARE specimen.

universal testing machine at a displacement rate of 0.05 mm/min. The pre-crack notch length was created by a saw with a new razor blade to obtain a sharp crack as shown in Figure 6(b). From the three-point bending tests, the fracture toughness K_{IC} in ($MPa \cdot m^{1/2}$) of SENB samples can be calculated using the following formulation [38]:

$$K_{IC} = \frac{P_I}{h\sqrt{w}} f(x) \tag{3}$$

$$f(x) = 6x^{0.5} \frac{[1.99 - x(1-x)(2.15 - 3.93x + 2.7x^2)]}{(1+2x)(1-x)^{3/2}} \tag{4}$$

where, P_I indicates the peak load, h is the specimen thickness, and x is a dimensionless value equal to crack length (a)/specimen (w). The fracture energy G_{IC} in terms of the material constants can be calculated as follows: where E is the Young's modulus and v is the Poisson's ratio equaling to 0.34.

$$G_{IC} = \frac{K_{IC}^2 (1 - v^2)}{E} \tag{5}$$

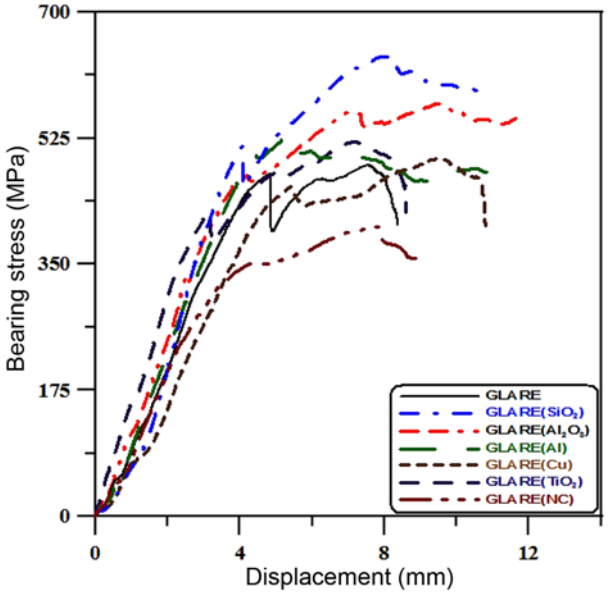

Figure 7. Bearing stress vs displacement curves of GLARE laminates filled with different nano-fillers.

Results and Discussion

Bearing Strength

Figure 7 shows bearing stress vs displacement curves of pristine GLARE and GLARE laminates filled with nano-fillers extracted from the bearing strength tests. The bearing strength increased nearly linearly with the displacement, and then significant non-linear behavior was observed in the bearing stress-displacement curve. The figure revealed that the bearing strength and displacement enhanced with GLARE (SiO_2), GLARE (Al_2O_3), GLARE (Al), GLARE (Cu), and GLARE (TiO_2). In the contrary, adding nanoclay to GLARE led to deterioration in bearing strength. A drop in the bearing stress-displacement curve of in pristine GLARE was clearly observed, whereas GLARE laminates filled with nano-fillers do not. A similar observation was observed by [23] for carbon fiber/epoxy composites reinforced with aligned carbon nanotube. The load drop in neat carbon fiber/epoxy composite is attributed to shear-dominated delamination developed between the plies. However, this load drop was not observed for nanocomposites as aligned carbon nanotube suppressed the delamination. Maximum improvement in bearing strength was obtained with GLARE filled with silica nano-fillers. Figure 8 shows the average bearing strength value of pristine GLARE and GLARE laminates filled with various nano-fillers. An enhancement of 26.3 %, 21.6 %, 12.3 %, 11.9 % and 3.2 % in bearing strength was obtained with GLARE (SiO_2), GLARE (Al_2O_3), GLARE (Al), GLARE (Cu), and GLARE (TiO_2), respectively. However, a decrease in bearing strength was obtained with the incorporation of NC nano-fillers compared to pristine GLARE.

Figure 9 shows the damage mechanism in pristine GLARE and GLARE laminates filled with nano-fillers subjected to tension bearing test. Bolt-bearing failure

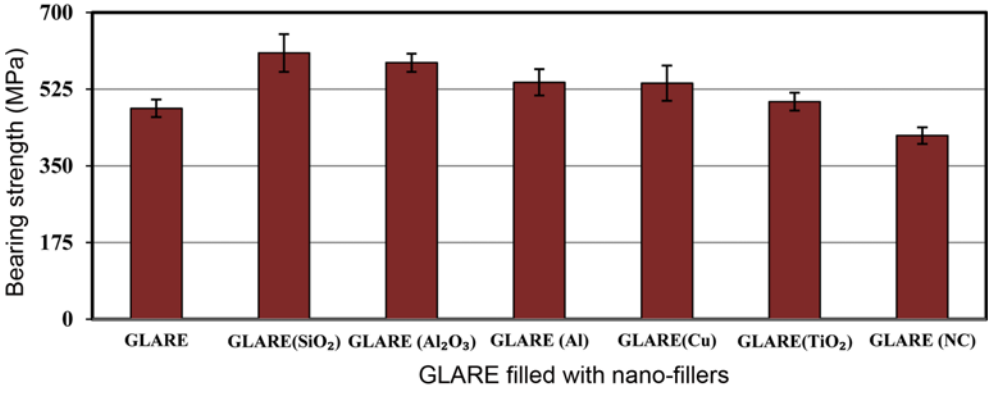

Figure 8. Bearing strength of GLARE laminates filled with different nano-fillers.

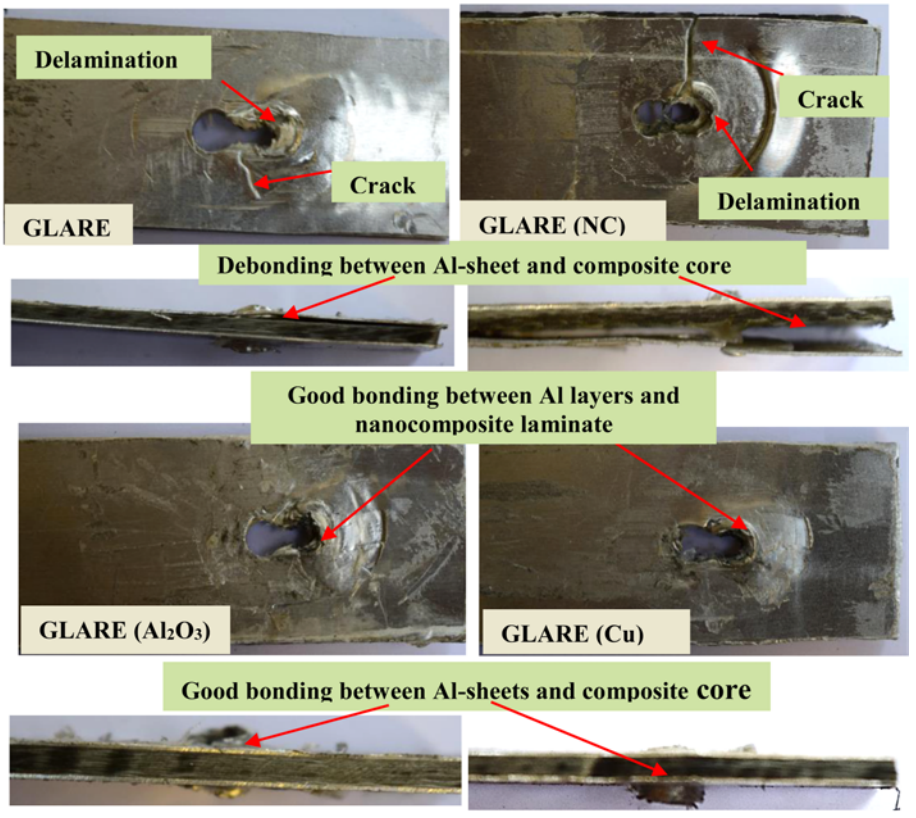

Figure 9. Damage mechanism in bolted GLARE laminates filled with different nano-fillers.

includes mechanisms as interlaminar delamination, fiber micro buckling, matrix cracking, and shear cracking [23]. As shown in pristine GLARE, clear delamination between the Al-skin layers and composite laminate was obtained around the hole after the failure occurred. A small crack propagated from the hole to the edge of the specimen on one side. However, in GLARE laminates filled with Al_2O_3 and Cu nanoparticles, nanocomposite laminate was perfectly bonded to the Al-metal layers around the hole indicating an improved adhesion between Al-layers and composite as compared to pristine GLARE. Slight delamination between nanocomposite layers was observed without separation between Al-layers and composite laminate around the hole. This revealed a good adhesion between nanofilled epoxy and glass fibers, which resulted in an improvement in bearing strength when compared to pristine GLARE. On the contrary, adding NC nano-fillers leads to separation and deterioration in the interfacial bond between Al-layers and nanocomposite laminate around the hole after fracture, which in turn decreases bearing strength as compared to pristine GLARE. Fracture occurring between woven glass fiber and nanofilled epoxy interface creates layer cracks in the composite core that act as initiation sites for delamination. The weak fiber-matrix interaction as well as the weak adhesion of NC nano-fillers in epoxy resin leads to lower stress transfer between epoxy resin, nano-fillers, and glass fiber. Moreover, the reduction in bearing strength is due to the nano-fillers agglomerations, where particle-particle interaction plays a major role as compared with particle-polymer matrix interaction. This NC nano-fillers aggregation causes defects in GLARE (NC) and acts as stress concentrations thus create cracks resulting in early failure. These aggregations possess a higher surface area that helps in the formation of enclosed air bubbles from the atmosphere. The enhancement in the bearing strength in nanocomposite laminates may be attributed to the good dispersion of nano-fillers in the epoxy matrix. To determine the distribution of Al_2O_3 nanoparticles in the nano-filled GLARE, surface analysis of GLARE filled with Al_2O_3 nano-fillers samples was explored by SEM and EDX images as shown in Figure 10. Surface scan showed a homogeneous distribution of elements in nano-filled GLARE. From Figure 10(b-e), it can be depicted that carbon covers almost the entire surface of the specimen. It is clear that Al and oxygen are present less in the samples. Also, it was indicated that a uniform distribution of Al_2O_3 nanoparticles into the epoxy matrix was observed. This proves the good dispersion and distribution attained through the sonication process during the fabrication of nanocomposites. The uniform distribution of Al_2O_3 nanoparticles in the composite core of GLARE revealed the enhancement in bearing strength

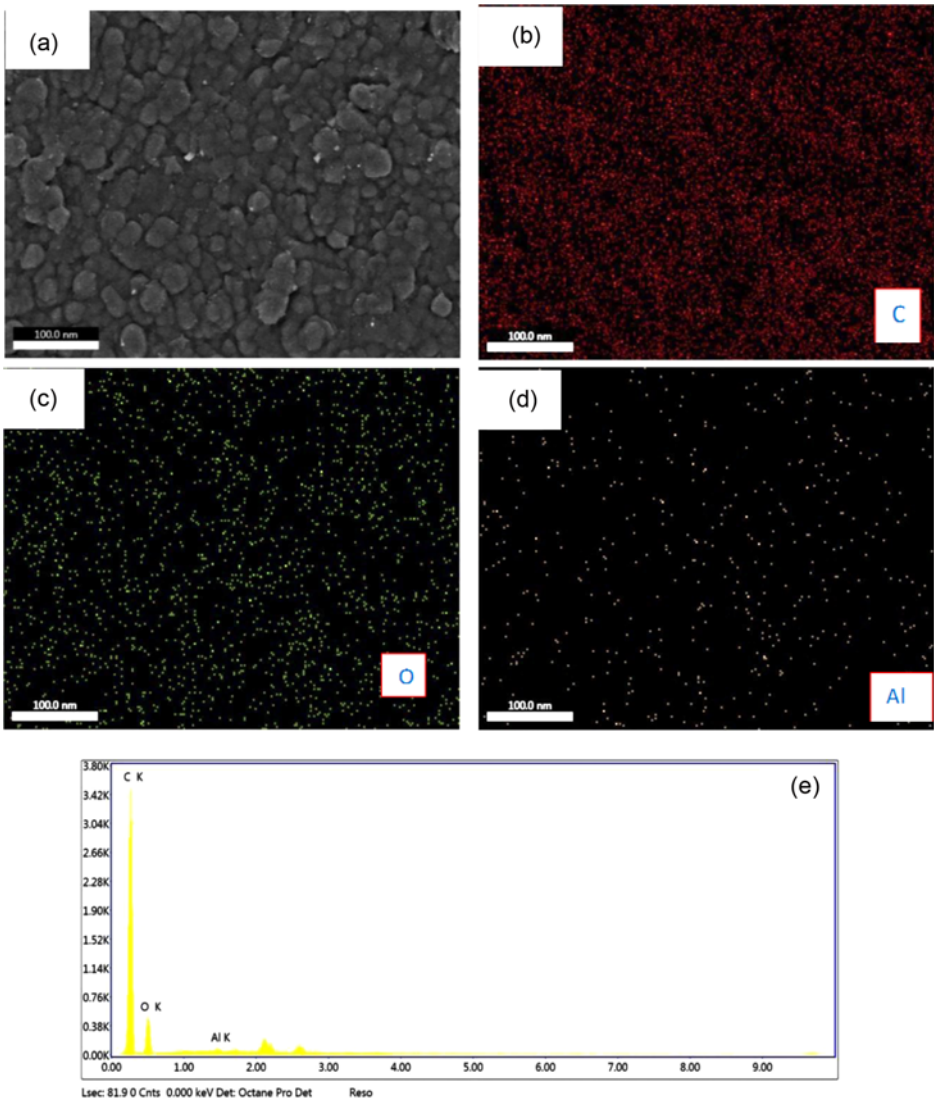

Figure 10. (a) FE-SEM of GLARE filled with Al_2O_3 nanoparticles, (b)-(d) elemental map, and (e) EDX.

of GLARE laminates.

In-plane Shear Strength

Figure 11 shows the in-plane shear stress vs displacement curves of pristine GLARE and GLARE laminates filled with nano-fillers. The in-plane shear stress-displacement curves show a nonlinear behavior until the maximum shear stress. The figure showed that the in-plane shear strength and displacement enhanced with GLARE (SiO_2), GLARE (Al_2O_3), GLARE (Al), GLARE (Cu), and GLARE (TiO_2). However, adding nanoclay to GLARE decreased the in-plane shear strength. Figure 12 shows the average in-plane shear strength values of pristine GLARE and GLARE laminates filled with nano-fillers. GLARE (SiO_2) exhibited the maximum enhancement of 35 % in in-plane shear strength as compared to pristine GLARE. Furthermore, an enhancement of 28.7 %, 19.5 %, 7.9 % and 5.3 % in in-plane shear strength was obtained with GLARE (Al_2O_3), GLARE (Al), GLARE (Cu), and GLARE (TiO_2), respectively. However, a reduction in in-plane shear strength was obtained with the incorporation of NC nano-fillers compared to pristine GLARE. The deterioration effect resulting from aggregation of NC nano-fillers and poor wetting behavior due to the high viscosity of epoxy [39]. Also, very high attractive forces between the particles, inducing a strong tendency to aggregate [40,41]. These aggregations possess a higher surface area that helps in the formation of enclosed air bubbles from the atmosphere. Hence, this results in a reduction in the mechanical properties of the polymeric nanocomposites [42]. The aggregations cause defects in the nanocomposite laminates and act as stress concentration that generates cracks that result in early failure.

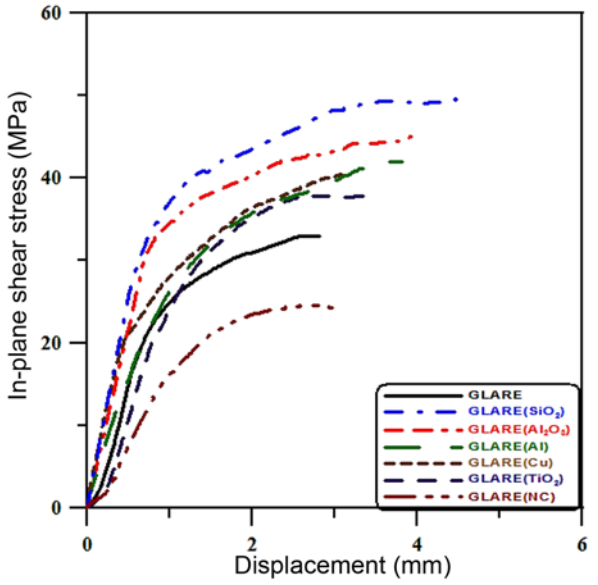

Figure 11. In-plane shear stress vs displacement curves of pristine GLARE and GLARE laminates filled with nano-fillers.

Figure 13 shows the damage mechanism in pristine GLARE and GLARE laminates filled with nano-fillers subjected to in-plane shear loads. As seen, crack started at the V-notch roots and grew to meet at the GLARE specimen center. In pristine GLARE, debonding between composite laminate and Al-skin layers indicates poor adhesion. However, in GLARE filled with Al_2O_3 nanoparticles, nanocomposite laminate is perfectly bonded to the Al-layers indicating improved adhesion compared to pristine GLARE. A similar observation was obtained for GLARE reinforced with SiO_2 nanoparticles. No delamination between nanocomposite layers was observed. This revealed the good adhesion between nanofilled epoxy and glass fibers which in turn increased the in-plane shear resistance as compared to pristine GLARE. In GLARE filled with Al-nanoparticles, the bonding between the nanocomposite and outer metal layers is not as perfect as the above-mentioned GLARE laminates filled with SiO_2 and Al_2O_3. Slight delamination between nanocomposite layers was observed. A similar observation was attained with GLARE reinforced with Cu nanoparticles. Polymer matrices filled with nano-fillers offer a more efficient stress transfer, which reduces the local stress concentration around the fiber/matrix interlayer, and improves the interfacial adhesion and mechanical performance of laminates [43]. On the contrary, adding NC nano-filler leads to more delamination i.e. deterioration in interfacial bond, which in turn decreases the in-plane shear strength.

Fracture Toughness

Fracture toughness is a very essential property for materials that determines the value of stress needed for a preexisting crack to propagate [28]. Figure 14 shows the fracture toughness values of pristine GLARE and GLARE laminates filled with various nano-fillers. A maximum improvement of 22.6 % in fracture toughness was obtained with GLARE filled with SiO_2 nano-filler. An enhancement of 20.7 %, 11.8 %, 10.5 %, and 5 % in fracture toughness was obtained with GLARE (Al_2O_3), GLARE (Al), GLARE (Cu), and GLARE (TiO_2), respectively. However, a decrease in fracture toughness was obtained with the incorporation of NC nano-fillers compared to pristine GLARE. That may be due to the tendency of NC to agglomerate. The agglomerations of nanoparticles can form a network through the whole polymer matrix and occlude the liquid polymer in their interparticle voids, thereby affecting the rheology of the composite underfill and giving a significant rise to the viscosity [44]. Figure 15 shows the fracture energy values of pristine GLARE and GLARE laminates filled with various nano-fillers. A maximum enhancement of 13.9 % was attained with GLARE filled with Al_2O_3 nanoparticles.

Figure 16 shows the damage mechanism in pristine GLARE and GLARE laminates filled with various nano-fillers subjected to fracture toughness test. As seen, in pristine GLARE, clear delamination between composite laminate layers occurred on the place of the upper support

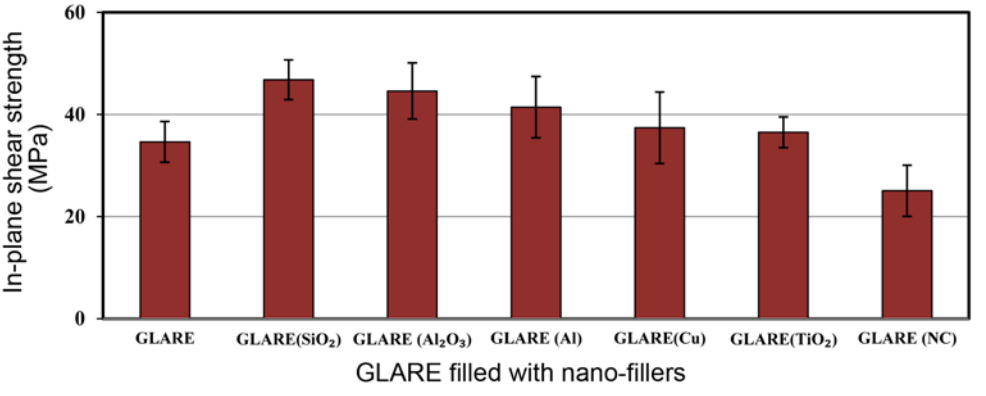

Figure 12. In-plane shear strength of pristine GLARE and GLARE laminates filled with nano-fillers.

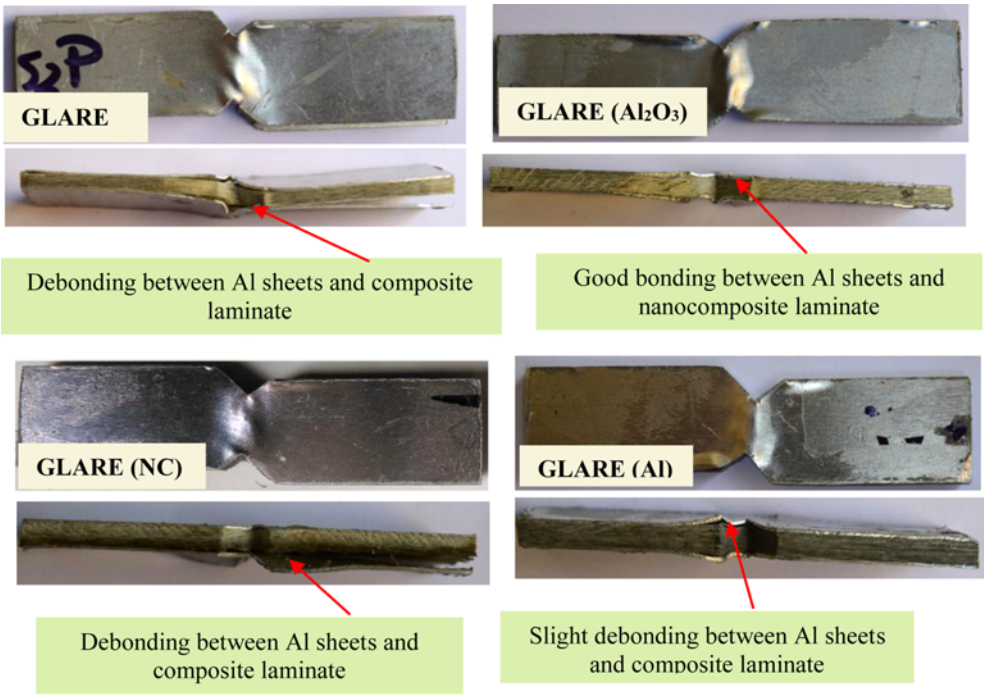

Figure 13. Damage mechanism in pristine GLARE and GLARE laminates filled with nano-fillers subjected to in-plane shear loads.

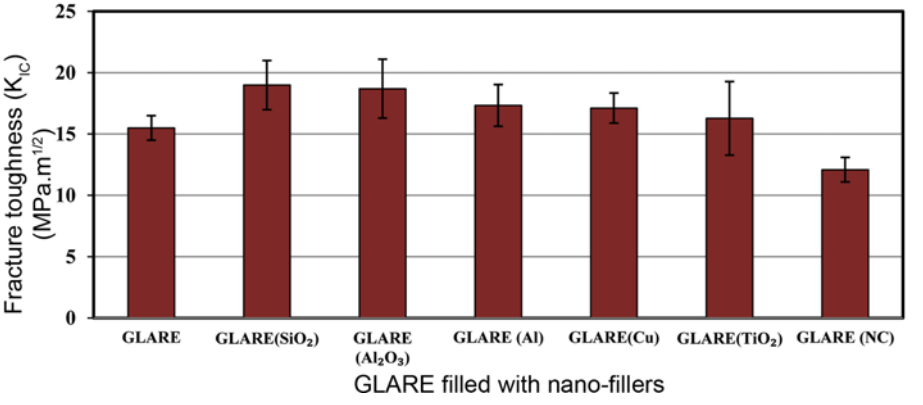

Figure 14. Fracture toughness of pristine GLARE and GLARE laminates filled with nano-fillers.

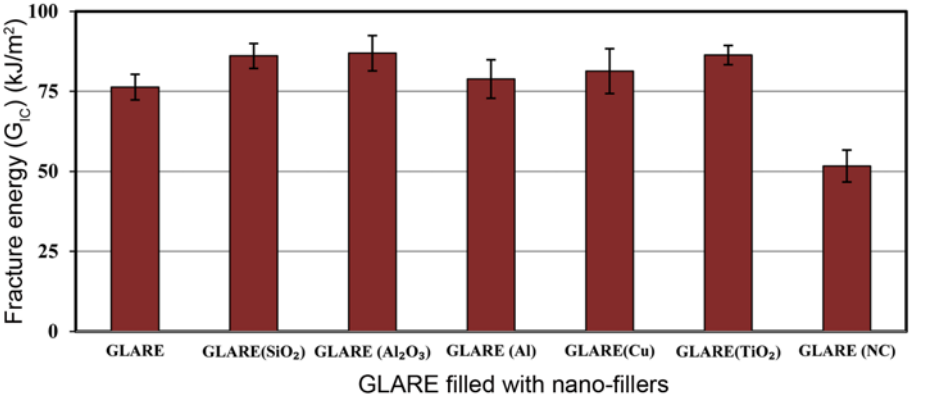

Figure 15. Fracture energy of pristine GLARE and GLARE laminates filled with nano-fillers.

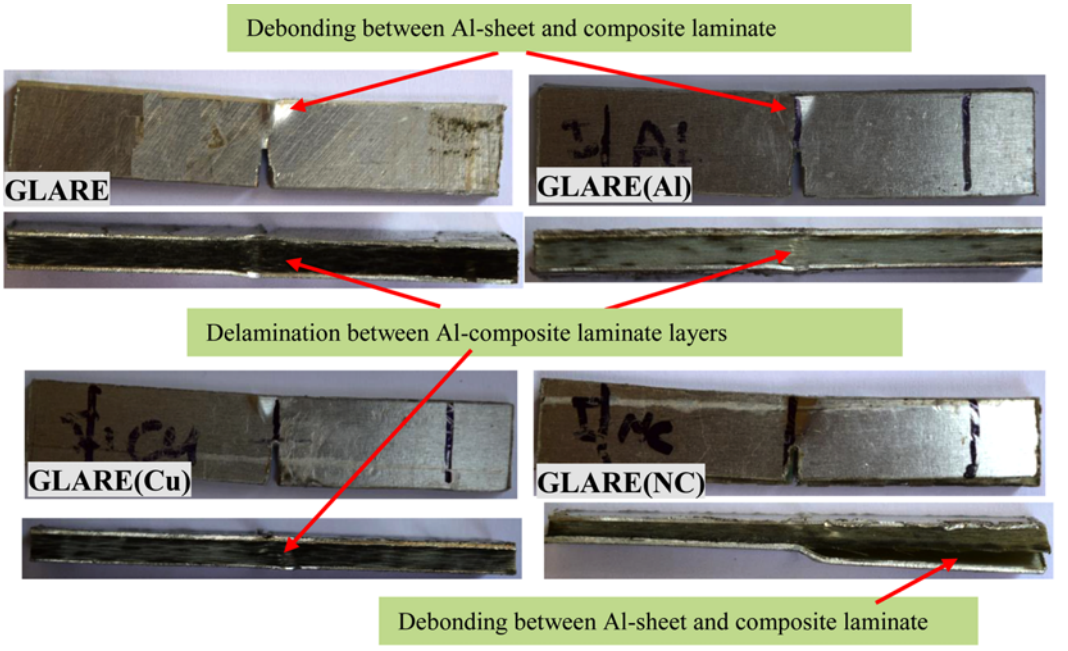

Figure 16. Damage mechanism of fracture toughness in pristine GLARE and GLARE laminates filled with nano-fillers.

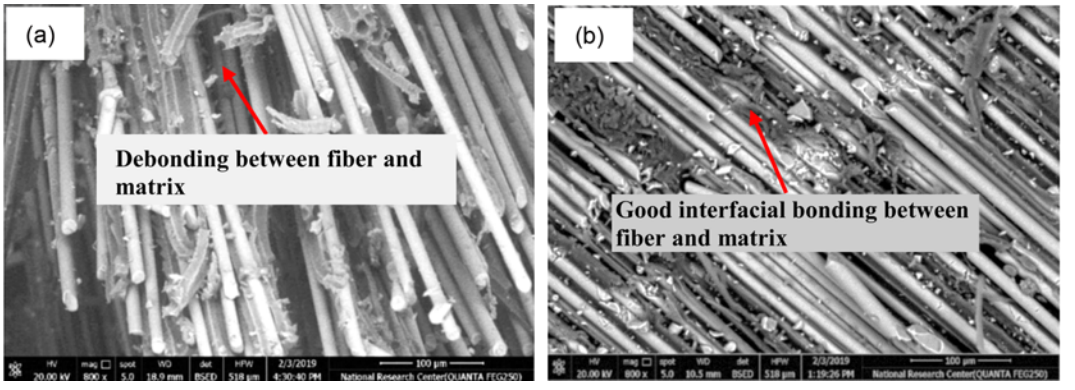

Figure 17. SEM images for fracture surface of (a) pristine GLARE and (b) GLARE laminates filled with nano-fillers subjected to fracture toughness test.

through the thickness of GLARE specimen. However, in GLARE filled with Al_2O_3 nanoparticles, the nanocomposite laminate was good adhered to Al-layers indicating an improved bonding between Al/nanocomposite as compared to pristine GLARE. A similar observation was obtained with GLARE reinforced with SiO_2 nanoparticles. Slight delamination between nanocomposite layers was observed on the place of the upper support through the thickness of the specimen. This revealed good adhesion between nanofilled epoxy and glass fibers, which resulted in an increase in the fracture toughness when compared to pristine GLARE. In GLARE filled with Cu nano-fillers, slight delamination between nanocomposite layers was observed without separation between Al-layers/composite laminate. A similar observation was attained with GLARE filled with Al nano-fillers. On the contrary, adding NC nano-fillers leads to separation and deterioration in the interfacial bond between Al-layers and nanocomposite laminate, which in turn decreased the fracture toughness as compared to pristine GLARE.

Figure 17 shows the SEM images of the fracture surface of pristine GLARE and GLARE filled with SiO_2 nano-fillers subjected to fracture toughness test. Poor adhesion was observed in pristine GLARE, thus a decrease in the fracture toughness was attained. However, good interfacial bonding was observed between fiber and SiO_2 nanofilled epoxy. The good interfacial bond orients the crack growth path through the nanophase matrix. This long traveling path of the propagation of crack consumes high energy and hence

improves the fracture toughness as compared to pristine GLARE.

Conclusion

In this work, an experimental study was carried out to evaluate the bearing strength, in-plane shear strength, and fracture toughness of pristine GLARE and GLARE laminates filled with various nano-fillers. Several types of nano-fillers were added to GLARE with 1 wt. % of epoxy. The following conclusions were drawn from this study:

1. Adding SiO_2, Al_2O_3, Cu, Al, and TiO_2 nano-fillers to GLARE enhanced the bearing strength, in-plane-shear, and fracture toughness as compared to pristine GLARE. On the contrary, adding NC to GLARE led to deterioration in bearing strength, in-plane-shear, and fracture toughness as compared to pristine GLARE.
2. An enhancement of 26.3 %, 21.6 %, 12.3 %, 11.9 % and 3.2 % in bearing strength was obtained with GLARE (SiO_2), GLARE (Al_2O_3), GLARE (Al), GLARE (Cu), and GLARE (TiO_2), respectively.
3. An enhancement of 35 %, 28.7 %, 19.5 %, 7.9 % and 5.3 % in in-plane shear strength was obtained with GLARE (SiO_2), GLARE (Al_2O_3), GLARE (Al), GLARE (Cu), and GLARE (TiO_2), respectively.
4. An enhancement of 22.6 %, 20.7 %, 11.8 %, 10.5 %, and 5 % in fracture toughness was obtained with GLARE (SiO_2), GLARE (Al_2O_3), GLARE (Al), GLARE (Cu), and GLARE (TiO_2), respectively.
5. The elemental map showed a uniform distribution of Al_2O_3 nano-fillers into the epoxy matrix. This proves the good dispersion and distribution attained through the sonication process during the fabrication of nanocomposites. The uniform distribution of Al_2O_3 nanoparticles in the composite core of GLARE revealed the enhancement in in-plane shear strength, and fracture toughness as compared to pristine GLARE.

References

1. M. Megahed, M. Abd El-baky, A. M. Alsaeedy, and A. E. Alshorbagy, *Compos. Part B-Eng.*, **176**, 107277 (2019).
2. W. J. Cantwell and P. Corte, *Compos. Sci. Technol.*, **66**, 2306 (2006).
3. T. Sinmazçelik, E. Avcu, M. Bora, and O. Çoban, *Mater. Des.*, **32**, 3671 (2011).
4. J. Ríos, E. Chomik, J. Balderrama, F. Cambiasso, and E. Asta, *Procedia Mater. Sci.*, **9**, 530 (2015).
5. M. Hagenbeek, C. Van Hengel, O. J. Bosker, and C Vermeeren, *Appl. Compos. Mater.*, **10**, 207 (2003).
6. M. Abouhamzeh, D. Nardi, R. Leonard, and J. Sinke, *Compos. Part A*, **114**, 258 (2018).
7. S. U. Khan, R. C. Alderliesten, and R. Benedictus, *Int. J. Fatigue*, **33**, 1292 (2011).
8. Y. Xiao and T. Ishikawa, *Compos. Sci. Technol.*, **65**, 1022 (2005).
9. F. Ascione, L. Feo, and F. Maceri, *Compos. Part B*, **40**, 197 (2009).
10. U. A. Khashaba, T. A. Sebaey, and K. A. Alnefaie, *Compos. Part B*, **45**, 1694 (2013).
11. O. Asi, *Compos. Struct.*, **92**, 35 (2010).
12. Y. Xiao, W. X. Wang, and Y. I. T. Takao, *J. Compos. Mater.*, **34**, 69 (2000).
13. F. Behrooz, M. Esmkhani, and A. Yaghoobi-Chatroodi, *Polym. Polym. Compos*., **28**, 159 (2019).
14. E. Totry, J. M. Molina-aldareguía, C. González, and J. Llorca, *Compos. Sci. Technol.*, **70**, 970 (2010).
15. C. Meola, A. Squillace, and L. Nele, *J. Compos. Mater.*, **37**, 1543 (2003).
16. D. R. Paul and L. M. Robeso, *Polymer*, **49**, 3187 (2008).
17. V. S. Nguyen, D. Rouxel, R. Hadji, B. Vincent, and Y. Fort, *Ultrason Sonochem*, **18**, 382 (2011).
18. E. T. Thostenson, C. Li, and T. Chou, *Compos. Sci. Technol.*, **65**, 491 (2005).
19. M. Megahed, A. A. Megahed, and M. A. Agwa, *Mater. Technol.*, **33**, 398 (2018).
20. M. Megahed, A. Fathy, D. Morsy, and F. Shehata, *J. Ind. Text.*, doi: 10.1177/1528083719874479 (2019).
21. M. A. Agwa, M. Megahed, and A. A. Megahed, *Polym. Adv. Technol.*, **28**, 1115 (2017).
22. A. A. Megahed, M. A. Agwa, and M. Megahed, *Polym. Plast. Technol. Eng*., **57**, 251 (2018).
23. R. G. De Villoria, P. Hallander, L. Ydrefors, P. Nordin, and B. L. Wardle, *Compos. Sci. Technol.*, **133**, 33 (2016).
24. M. Attar, S. Ahmadpour, S. Banisadr, A. Mohammadi, S. Mirmoradi, and Z. Shirazi, *J. Mech. Sci. Technol.*, **33**, 2769 (2019).
25. K. Singh, C. J. S. Saini, and J. Brazilian, *Soc. Mech. Sci. Eng.*, **40**, 1 (2018).
26. H. Kim, *Met. Mater. Int.*, **21**, 185 (2015).
27. J. Cho, J. Y. Chen, and I. M. Daniel, *Scr. Mater.*, **56**, 685 (2007).
28. U. A. Khashaba, *Polym. Compos.*, **39**, 815 (2018).
29. H. Ulus, H. Kaybal, V. Eskizeybek, and A. Avci, *Fiber. Polym.*, **20**, 2184 (2019).
30. J. Tsai, H. Hsiao, and Y. Cheng, *J. Compos. Mater.*, **44**, 505 (2010).
31. A. Z. Zakaria, *Eng. Fract. Mech.*, **186**, 436 (2017).
32. J. Hundley, H. Hahn, J. Yang, and A. Facciano, *J. Compos. Mater.*, **45**, 751 (2010).
33. A. Z. Zakaria, K. Shelesh-nezhad, T. N. Chakherlou, and A. Olad, *Eng. Fract. Mech.*, **172**, 139 (2018).
34. M. R. Loos, L. A. F. Coelho, and S. H. Pezzin, *P. Ciência e Tecnol.*, **18**, 76 (2008).
35. A. Zakaria and K. Shelesh-nezhad, *Eng. Fract. Mech.*, **186**, 436 (2017).
36. A. Atas, G. F. Mohamed, and C. Soutis, *Compos. Sci. Technol.*, **72**, 1096 (2012).

37. M. McCarthy, V. Lawlor, W. Stanley, and C. McCarthy, *Compos. Sci. Technol.*, **62**, 1415 (2002).
38. J. L. Tsai, B. H. Huang, and Y. L. Cheng, *J. Compos. Mater.*, **43**, 3107 (2009).
39. L. L. Zhai, G. P. Ling, and Y. W. Wang, *Int. J. Adhes. Adhes.*, **28**, 23 (2008).
40. M. H. Wichmann, J. Sumfleth, F. H. Gojny, M. Quaresimin, B. Fiedler, and K. Schulte, *Eng. Fract. Mech.*, **73**, 2346 (2006).
41. A. Anand, R. Harshe, and M. Joshi, *J. Compos. Mater.*, **47**, 2937 (2013).
42. M. A. Ashraf, W. Peng, Y. Zare, and K. Y. Rhee, *Nanoscale Res. Lett*., **13**, 214 (2018).
43. Y. Tian, H. Zhang, and Z. Zhang, *Compos. Part A*, **98**, 1 (2017).
44. K. L. Kuzmin, I. A. Timoshkin, S. I. Gutnikov, E. S. Zhukovskaya, Y. V. Lipatov, and B. I. Lazoryak, *Compos. Interfaces*, **24**, 13 (2017).